Journal of
Mechanics of
Materials and Structures

NONLINEAR IMPACTING OSCILLATIONS OF PIPE CONVEYING PULSATING FLUID SUBJECTED TO DISTRIBUTED MOTION CONSTRAINTS

Wang Yikun, Ni Qiao, Wang Lin, Luo Yangyang and Yan Hao

msp

NONLINEAR IMPACTING OSCILLATIONS OF PIPE CONVEYING PULSATING FLUID SUBJECTED TO DISTRIBUTED MOTION CONSTRAINTS

WANG YIKUN, NI QIAO, WANG LIN, LUO YANGYANG AND YAN HAO

The nonlinear dynamics of a simply supported pipe conveying pulsating fluid is investigated by introducing distributed motion constraints along the pipe axis. The constraints are modeled by trilinear springs. The flowing fluid in the pipe is pulsatile, which is assumed to have a time-dependent harmonic component superposed on the steady fluid flow. Attention is concentrated on the potential performance of the pipe/impacting system with various pulsating frequencies. To investigate the short-wave buckling, the behaviors of the simply supported pipe with steady internal flow velocities are presented first. The partial differential equations (PDEs) are formulated and then transformed into a set of ordinary differential equations (ODEs) using the Galerkin's method. The nonlinear dynamical responses are presented in the form of bifurcation diagrams, time histories, phase portraits, Poincaré maps and power spectrums. Some interesting and sometimes unexpected results have been observed under various system parameters.

1. Introduction

The dynamical problem of pipes conveying fluid is an important academic topic with broad industrial applications, e.g., pump discharge lines, oil pipelines, propellant lines, reactor system components, microfluidic devices and so forth [Païdoussis 1998; Hu et al. 2016; Wang et al. 2016]. Their oscillation behavior is also one of the most troublesome problems in engineering applications. These industries usually utilize high thermal efficiency shell and heat exchanger designs to avoid failure. Some practical cases often require the devices to be able to work with high flow velocities, which in turn could cause pipes to experience complicated flow-induced vibrations.

A large number of studies have been devoted to the flow-induced vibrations of pipes due to their rich dynamical behavior [Païdoussis 1983; Chen 1991; Weaver et al. 2000; Pettigrew et al. 1978; Dai et al. 2014a]. Many researchers focused on the flow-induced vibrations of pipes to get better understanding of the mechanisms of the system. Studies related to this topic seem to have started in the 1960s. The stabilities and nonlinear dynamics of pipes conveying fluid were investigated both theoretically and experimentally. A very comprehensive introduction to the flow-induced vibrations and the associated linear stability problems can be found in [Chen 1987]. Nonlinear behaviors of slender structures subjected to axial fluid flows were discussed in details in [Païdoussis 1998]. Indeed, the pipe system exhibits a wide range of interesting dynamical behaviors under different boundary conditions and motion constraints. These cases cover a number of factors, such as the parametric excitations in the form of flow fluctuation, external excitations, various loose supports, articulated or continuous configuration, additional system

configurations like lumped mass, attached nozzles, elastic foundations, elastic constraints, and various forms of nonlinearities in the system arising from different aspects.

In the literature many studies have considered either pulsating fluid flows or motion constraints at one or finite number of locations on the pipe. The dynamics of a pipe conveying fluid was explored when the flow velocity is harmonically perturbed about a mean value in [Païdoussis and Sundararajan 1975]. Cantilevered and clamped-clamped models were investigated, in which the parametric and combination resonances were included. The method of averaging is adapted to examine the nonlinear dynamics of supported pipes conveying pulsating fluid in the vicinity of subharmonic resonances in [Sri Namachchivaya 1989; Chen 1971]. Several other notable papers on linear analytical models for these parametric instability problems of simply supported pipes were conducted in [Païdoussis and Issid 1974; Ginsberg 1973; Ariaratnam and Sri Namachchivaya 1986]. They have studied the parametric and combination resonances and evaluated the instability regions using Bolotin's method and numerical Floquet analysis. The nonlinear dynamics of supported pipes conveying pulsating fluid were discussed in [Sri Namachchivaya 1989; Jayaraman and Narayanan 1996; Chang and Chen 1994; Yoshizawa et al. 1986; Dai et al. 2014b]. From these studies, it is clear that the basic system of a pipe conveying pulsating fluid could lose stability at sufficiently high flow velocities. Thus, the analysis of subharmonic and combination resonances was the main interest for simply supported pipes conveying pulsating fluid, yielding the stability boundaries in the parameter space. For a perspective on the whole field of pipes conveying pulsating fluid, the interested reader is referred to [Païdoussis 1998].

In [Panda and Kar 2007; 2008; Wang 2009], a simply supported pipe conveying pulsating fluid was analyzed, in which the nonlinear force considered is associated with the axial extension of the pipe. By accounting for the nonlinearity resulted from the pipe's mean axial extension, the combination, principal parametric and internal resonances of supported pipes were investigated in the first two of these references. Nonlinear analysis of a cantilevered pipe conveying steady fluid with motion constraints was conducted in [Païdoussis and Semler 1993]. Two impact models representing the effect of motion constraints, i.e., cubic and trilinear springs, were introduced in the physical model and taken into account when deriving the nonlinear equation of motion. Results were obtained numerically in the form of bifurcation diagrams, phase plots, power spectral diagrams and time traces. Hassan et al. [2005] provided a means of representing the restraining force by a combination of edge and segmental contacts. The location of the contact segment during impact was unknown and determined artificially according to the researchers' interests in their studies. The location of the contact segment may greatly affect the performance of the system. The nonlinear dynamics of a simply supported pipe conveying pulsating fluid was further studied in [Wang 2009] by considering the effect of motion constraints modeled by cubic springs; the mean value of the pulsating velocity was assumed to be higher than the critical one for buckling instability, compared to the lower values of mean flow velocity used by [Sri Namachchivaya 1989; Sri Namachchivaya and Tien 1989]. Quasiperiodic and chaotic motions were obtained by using the Galerkin method with a two-mode approximation ($N = 2$). In [Xia and Wang 2010], an improved theoretical model for the dynamics of tube arrays subjected to cross flow was developed, with consideration of the nonlinearity associated with the mean axial extension of the tube array. The restraining forces were modeled either by cubic or trilinear springs. In [Tang et al. 2014] another theoretical model was developed to analyze the fluid-elastic vibration of a single flexible curved pipe, surrounded by rigid cylinders and subjected to cross-flow as well as loose supports.
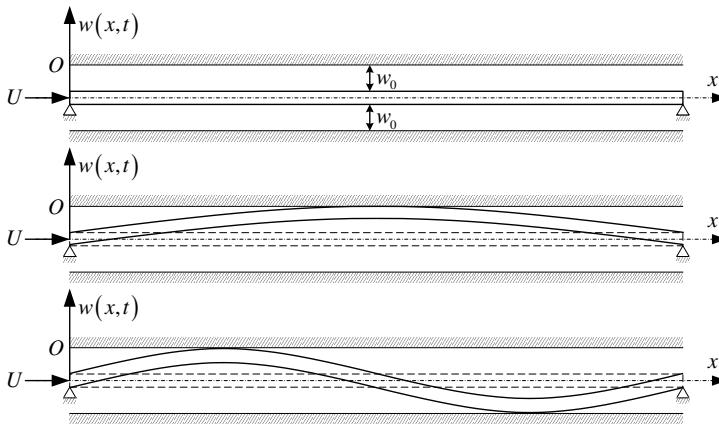
Figure 1. Schematic of the simply supported pipe conveying pulsating fluid with distributed motion constraints.
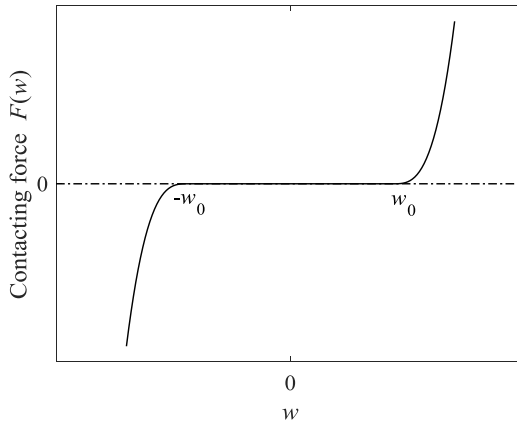
The present study initiates to investigate the dynamics of simply supported pipes with both internal pulsating fluid flow and distributed motion constraints imposed on the pipe. The simply supported pipe would impact the distributed motion constraints once the oscillation amplitude becomes sufficiently large. The constraints are modeled as trilinear springs and further improved as distributed constraints acting on the pipe along its axis. The pulsating internal flow has a time-dependent harmonic component superposed on the steady flow, such that $u = u_0(1 + \sigma \sin \omega\tau)$, where u_0 is the mean flow velocity of the internal fluid, σ is the pulsating amplitude, and ω is defined as the pulsating frequency of internal fluid flow. Particular attention is focused on the possible behaviors of the system by varying the values of pulsating frequencies of the unsteady internal fluid. Some interesting and sometimes unexpected results will be shown. The bifurcation diagrams, phase portraits, Poincaré maps and power spectral density diagrams will be constructed to present the dynamical behavior of the pipe system.

2. Equations of motion

In the current work, the simply supported pipe conveying pulsating fluid in the presence of distributed motion constraints is of length L, cross section area A, flexural rigidity EI, density ρ_p, mass per unit length m and coefficient of visco-elastic damping E^*. The internal flowing fluid is of density ρ_f, mass per unit length M and flow velocity U. The distributed motion constraints are modeled by trilinear springs along the pipe axis, as depicted in Figure 1.

The governing equation of a simply supported pipe in the absence of motion constraints has been obtained before [Panda and Kar 2007; Panda and Kar 2008; Jin and Song 2005]. The governing equation will be modified here to describe the behavior of the pipe with motion constraints. It is

$$EI\frac{\partial^4 w}{\partial x^4} + E^*I\frac{\partial^5 w}{\partial t\,\partial x^4} + 2MU\frac{\partial^2 w}{\partial t\,\partial x} + (M+m)\frac{\partial^2 w}{\partial t^2}$$
$$+ \left[MU^2 + M\frac{\partial U}{\partial t}(l-x) - \left(E + E^*\frac{\partial}{\partial t}\right)\frac{A}{2l}\int_0^l \left(\frac{\partial w}{\partial x}\right)^2 dx\right]\frac{\partial^2 w}{\partial x^2} + F(w) = 0, \quad (1)$$

Figure 2. Diagrammatic view of the contacting force $F(w)$ vs. the transverse displacement w.

in which $F(w)$ represents the effect of the nonlinear motion constraints acting on the pipe. Following [Païdoussis and Semler 1993], the nonlinear restraining force is given by

$$F(w) = K\big(w - \tfrac{1}{2}(|w + w_0| - |w - w_0|)\big)^3, \tag{2}$$

in which w_0 is the free gap between the pipe wall and the edge of the motion constraints; K is the stiffness of the trilinear springs. As suggested by [Païdoussis and Semler 1993], this expression of nonlinear force $F(w)$ agrees well with the experimental tests. A qualitative relation of the nonlinear spring force and the transverse displacement w is shown in Figure 2. There is no contact when $|w| < w_0$ and there is nonzero restraining force once $|w| > w_0$.

Introducing the following nondimensional quantities,

$$\eta = \frac{w}{L}, \quad \xi = \frac{x}{L}, \quad d = \frac{w_0}{L}, \quad \tau = \sqrt{\frac{EI}{m+M}}\frac{t}{L^2}, \quad u = \sqrt{\frac{M}{EI}}LU, \quad k = \frac{K_{spr}L^5}{EI},$$

$$\alpha = \sqrt{\frac{EI}{m+M}}\frac{E^*}{L^2}, \quad \beta = \frac{M}{m+M}, \quad \kappa = \frac{AL^2}{2I}$$

Equation (1) can be rewritten in a dimensionless form as

$$\begin{aligned}
&\alpha\frac{\partial^5\eta}{\partial\tau\,\partial\xi^4} + \frac{\partial^4\eta}{\partial\xi^4} + \big[u^2 + \sqrt{\beta}\dot{u}(1-\xi)\big]\frac{\partial^2\eta}{\partial\xi^2} + 2\sqrt{\beta}u\frac{\partial^2\eta}{\partial\tau\,\partial\xi} + \frac{\partial^2\eta}{\partial\tau^2}\\
&-\kappa\frac{\partial^2\eta}{\partial\xi^2}\int_0^1\Big(\frac{\partial\eta}{\partial\xi}\Big)^2 d\xi - 2\alpha\kappa\frac{\partial^2\eta}{\partial\xi^2}\int_0^1\frac{\partial\eta}{\partial\xi}\frac{\partial^2\eta}{\partial\tau\,\partial\xi}d\xi + f(\eta) = 0.
\end{aligned} \tag{3}$$

The nondimensional restraining force is expressed as

$$f(\eta) = k\big(\eta - \tfrac{1}{2}(|\eta+d| - |\eta-d|)\big)^3. \tag{4}$$

The nondimensional pulsating fluid velocity is described by a sinusoidal fluctuation in τ:

$$u = u_0(1 + \sigma \sin\omega\tau), \tag{5}$$

where u_0 is the mean flow velocity, σ is the pulsating magnitude and ω the pulsating frequency.

The infinite dimensional model can be discretized via Galerkin's technique, with the simply supported beam eigenfunctions $\phi_j(\xi)$. These eigenfunctions are used as a suitable set of base functions with $q_j(\tau)$ being the corresponding generalized coordinates; thus

$$\eta(\xi, \tau) = \sum_{j=1}^{N} \phi_j(\xi) q_j(\tau), \tag{6}$$

where N is the number of modes taken into calculations. Substituting (6) into (3), multiplying by $\phi_i(\xi)$ and integrating from 0 to 1 leads to

$$\{\ddot{q}\} + [C]\{\dot{q}\} + [K]\{q\} + \{f(q)\} + \{g(q, \dot{q})\} = \{0\}. \tag{7}$$

$[C]$, $[K]$, $\{f(q)\}$ and $\{g(q, \dot{q})\}$ represent the stationary damping and stiffness matrices, column vectors of the nonlinear restraining forces and geometrically nonlinear terms, respectively. The elements of $[C]$, $[K]$, $\{f(q)\}$ and $\{g(q, \dot{q})\}$ are given by

$$C_{ij} = \alpha c_{ij}^1 + 2\sqrt{\beta} u_0 (1 + \sigma \sin \omega\tau) c_{ij}^2, \quad K_{ij} = k_{ij}^1 + u_0^2 (1 + \sigma \sin \omega\tau)^2 k_{ij}^2 + \sqrt{\beta} u_0 \sigma \omega \cos \omega\tau k_{ij}^3,$$

$$f_i = \int_0^1 \phi_i(\xi) f\left(\sum_{j=1}^{N} \phi_j(\xi) q_j\right) d\xi, \qquad g_i = g_{ijkl}^1 q_j q_k q_l + g_{ijkl}^2 q_j q_k \dot{q}_l, \tag{8}$$

where

$$c_{ij}^1 = \lambda_i^4 \delta_{ij}, \quad c_{ij}^2 = \int_0^1 \phi_i \phi_j' d\xi, \qquad k_{ij}^1 = \lambda_1 \delta_{ij}, \quad k_{ij}^2 = -\lambda_i^2 \delta_{ij}, \quad k_{ij}^3 = \int_0^1 (1 - \xi) \phi_i \phi_j'' d\xi,$$

$$g_{ijkl}^1 = g_{ijkl}^2 = \int_0^1 \phi_1 \phi_j'' \int_0^1 \phi_k' \phi_l' d\xi d\xi. \tag{9}$$

The calculation of the values of f_i in (8) deserves special attention. As can be seen in (4), the impacting force $f(\eta)$ is a function of η. In the numerical algorithm, the values of $q_i(\tau)$ for arbitrary time τ can be calculated from (7) provided that the initial conditions were given, and then the displacement $\eta(\xi, \tau)$ is obtained using (6). The instantaneous values of $\eta(\xi, \tau)$ are further substituted into (4), yielding the values of distributed impacting force along the pipe axis at that time. Finally, the values of f_i can be obtained using the third expression of (8). The interested reader can get the matrix forms of the other coefficients (C_{ij}, K_{ij}, g_i) from [Ni et al. 2015]. For the purpose of numerical computation, we define $p = \dot{q}$ and $z = [q; p]$; equation (9) is then reduced to its first-order form:

$$\dot{z} = Az + F + G, \tag{10}$$

where

$$A = \begin{bmatrix} \mathbf{0} & \mathbf{I} \\ -\mathbf{K} & -\mathbf{C} \end{bmatrix}, \quad G = \begin{bmatrix} \mathbf{0} \\ -g \end{bmatrix}, \quad F = \begin{bmatrix} \mathbf{0} \\ -f \end{bmatrix}. \tag{11}$$

It follows from (10) that A, G and F are $2N \times 2N$, $2N \times 1$ and $2N \times 1$ matrices, respectively.

3. Results and discussion

In the following, the dynamical behaviors of the simply supported pipe conveying pulsating fluid with distributed motion constraints will be investigated numerically. To the author's knowledge, the nonlinear responses of a supported pipe conveying pulsating fluid with relatively high mean flow velocity in the presence of distributed motion constraints have not yet been explored. Therefore, we analyze the nonlinear vibrations of hinged–hinged pipes conveying fluid regarding this topic.

As is known that for a simply-supported pipe conveying fluid with a steady flow velocity, divergence in the first mode occurs at a dimensionless critical flow velocity $u_c = \pi$ [Païdoussis 1998]. The main aim of this paper is to explore the effects of the pulsating frequency ω with higher mean flow velocity u_0 and the introduction of distributed motion constraints. For that reason, solutions of (10) are obtained by using the fourth-order Runge–Kutta method, with the following initial conditions employed, $z(1) = \cdots = z(N) = -0.001$ and $z(N+1) = \cdots = z(2N) = 0$.

The results to be presented are obtained with $N = 4$ since this choice is sufficient for predicting the nonlinear responses of supported pipes, provided that the pulsating frequency is relatively small [Ni et al. 2014]. In the following calculations, some of the physical parameters are chosen to be

$$\alpha = 0.005, \quad \beta = 0.64, \quad \kappa = 5000, \quad k = 5.6 \times 10^6, \quad d = 0.044, \quad \sigma = 0.4. \tag{12}$$

3.1. *Validation of the algorithm.* In order to illustrate the effectiveness of the present algorithm, we first consider the model of a simply supported pipe conveying pulsating fluid without motion constraints. The system parameters are selected to be those used in [Wang 2009; Ni et al. 2014], i.e., $\alpha = 0.005$, $\beta = 0.64$ and $\kappa = 5000$. The mean flow velocity is chosen to be $u_0 = 4.5$ and the pulsating amplitude is $\sigma = 0.4$. It is noted that the bifurcation diagram for $N = 2$ shown in Figure 3 without motion constraints are in good agreement with those obtained in those references. This validates the correctness of the present numerical scheme used in the following analysis.
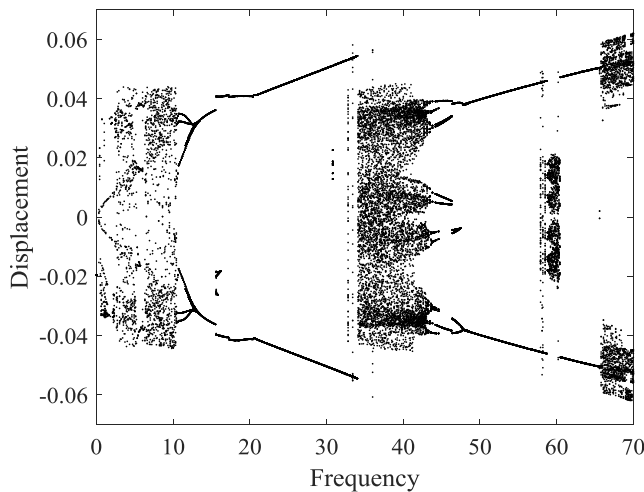
Figure 3. Bifurcation diagram of the mid-point displacement, for $N = 2$, $u_0 = 4.5$, $\sigma = 0.4$, $\alpha = 0.005$, $\beta = 0.64$ and $\kappa = 5000$.

3.2. *Buckling of the pipe with motion constraints for $\sigma = 0$ and $\omega = 0$.* To investigate the static short-wave buckling, results will be presented first with the flow velocity assumed to be constant. The pipe is placed between the two-sided motion constraints, which are described by a trilinear-spring contact model. As mentioned in the foregoing, [Ni et al. 2014] have proved the effectiveness of the truncating number $N = 4$ in the presence of nonlinear motion constraints. So, the buckling analyses are conducted by truncating (8) at $N = 4$. To get a good understanding of the buckling style, bifurcation diagrams for displacements of three points on the pipe will be performed, i.e., for $\eta(0.25, \tau)$, $\eta(0.5, \tau)$ and $\eta(0.75, \tau)$. That is, whenever the oscillation velocity is zero (i.e., $\dot{\eta}(0.25, \tau)$, $\dot{\eta}(0.5, \tau)$ or $\dot{\eta}(0.75, \tau)$ are equal to zero), the corresponding displacement will be recorded.

Numerical results shown in Figure 4 are based on the trilinear-spring model. Inspecting Figure 4, it is easy to find that, with the increasing of flow velocity, the pipe exhibits different types of buckling instability. For $0 < u_0 < 3.14$, the pipe stays at the equilibrium position. This is because the flow-induced effect cannot overcome the damping effect of the system. For $3.15 < u_0 < 15.7$, the pipe is buckled with a half-wave configuration. However, as u_0 is further increased, the half-wave configuration becomes flatter in the vicinity of peak displacement, which means more and more parts of the pipe tend to contact the motion constraints. In this case, the contact ratio between the pipe and the distributed motion constraints becomes larger. The restraining force acts on the pipe and cuts the wave crest of the buckling configuration. The configuration of the pipe is symmetrical although it is not exactly a sinusoidal one. For $15.8 < u_0 < 19.7$, the pipe along the axial direction behaves like a "W" shape. Interestingly, the two half-waves occur at the same side of the straight equilibrium position. Moreover, another region of $19.8 < u_0 < 25$ generates a buckling shape similar to the curve of one period of a sinusoidal function. Several typical buckling configurations of the pipe for various flow velocities are shown in Figure 5. These results show the significant influence of motion constraints on the behavior of the pipe system.
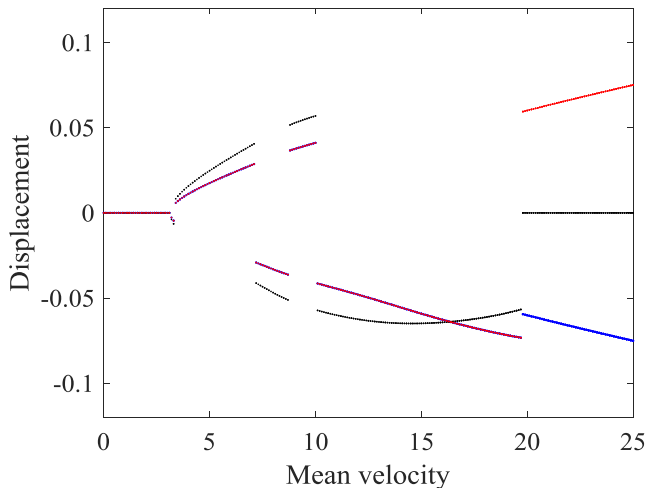
Figure 4. Bifurcation diagram for $\eta(0.25, \tau)$ (blue), $\eta(0.5, \tau)$ (black) and $\eta(0.75, \tau)$ (red), as the mean velocity u_0 varies. (Overlapping red and blue points when $u_0 < 19.7$ indicate symmetry of the pipe shape).
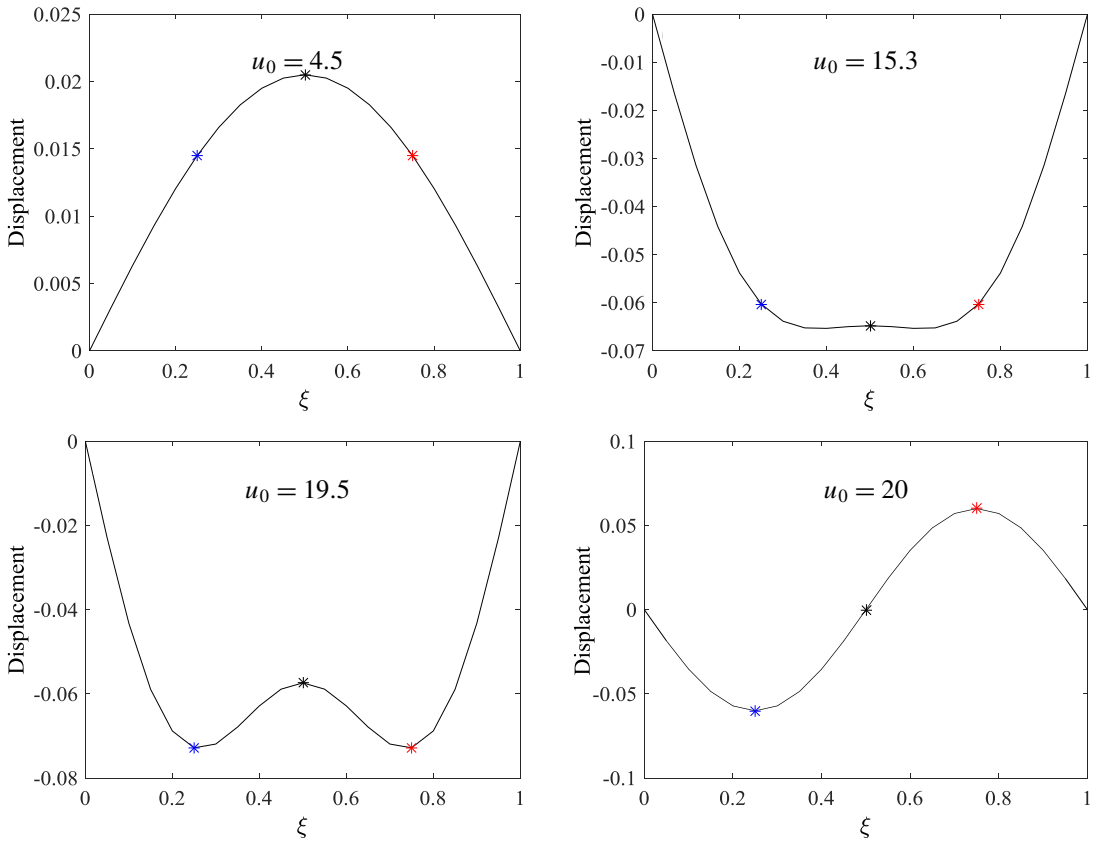
Figure 5. Buckling configurations of the pipe conveying steady fluid flow for various flow velocities u_0.

3.3. *Responses of the pipe with pulsating internal flows.* In this subsection, the effects of pulsating internal flows on the responses of the pipe system will be explored. As mentioned in the foregoing, in some working conditions, the mean flow velocity may be much higher than $u_c = \pi$. Therefore, in this paper, the flow velocity is chosen to be higher than u_c. We consider the cases of $u_0 = 4.5$ and $u_0 = 6$, respectively. Bifurcation diagrams for the midpoint displacement of the pipe are conducted, as the pulsating frequency ω is varying.

It can be seen from Figure 6 that, for $u_0 = 4.5$ and $0 < \omega < 20$, the dynamics of the pipe/impacting system are similar to those of the pipe in the absence of motion constraints. This can be expected since the vibration amplitude of the mid-point of the pipe does not exceed the gap of the motion constraints in such case. Moreover, the contact force is small at the onset of impacting. Thus, in the range of $0 < \omega < 20$, the pipe has an occurrence of 'free flight' between the two-sided constraints. And periodic motions are detected in the range of $20 < \omega < 38.7$. Compared with the amplitude shown in Figure 3, the displacement amplitude is limited to be smaller and is slightly larger than the gap distance, indicating that contact between the motion constraints and pipe occurs. The oscillation of the pipe further evolves to become chaotic for $\omega > 38.8$, while for a pipe without motion constraints the threshold for chaos is about $\omega = 32.8$. In fact, in the range of $\omega > 38.8$, quasiperiodic motion might also occur.
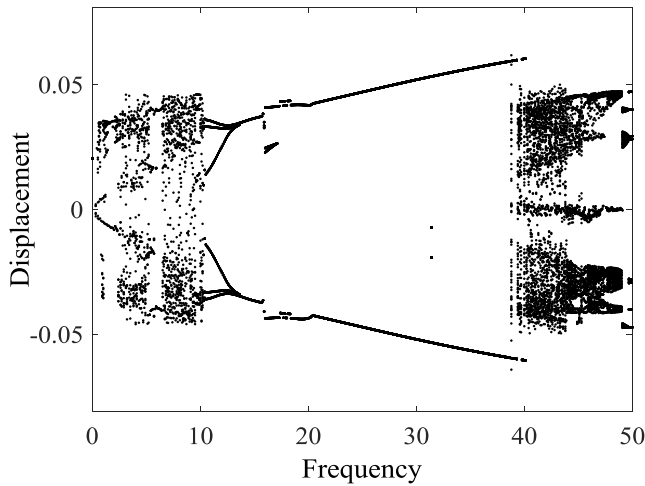
Figure 6. Bifurcation diagram for the constrained pipe system with $u_0 = 4.5$ at $\xi = 0.5$.
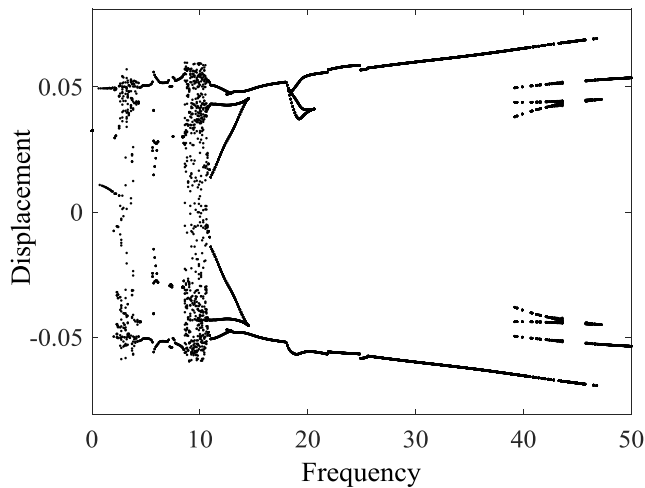
**Figure 7.** Bifurcation diagram for the constrained pipe system with $u_0 = 6$ at $\xi = 0.5$.

Considering the case with relatively high mean flow velocity, i.e., $u_0 = 6$, a quite different result is obtained, as presented in Figure 7. For $u_0 = 6$, impact between the pipe and constraints would occur for all pulsating frequencies considered, since the displacement amplitude in the absence of constraints reaches at a value of 0.494, which is larger than the gap distance between the pipe and constraints. As the pulsating frequency increases, it follows from Figure 7 that the response of the pipe may be periodic, quasiperiodic or chaotic. When the pulsating frequency is larger than $\omega = 10.9$, different types of periodic motion (with periods 1, 2 and 3) might occur.

Sample results of phase plots and power spectral density diagrams for the system with $u_0 = 4.5$ and $u_0 = 6$ are further presented in Figures 8 and 9. It can be seen that the pipe vibrates regularly or irregularly
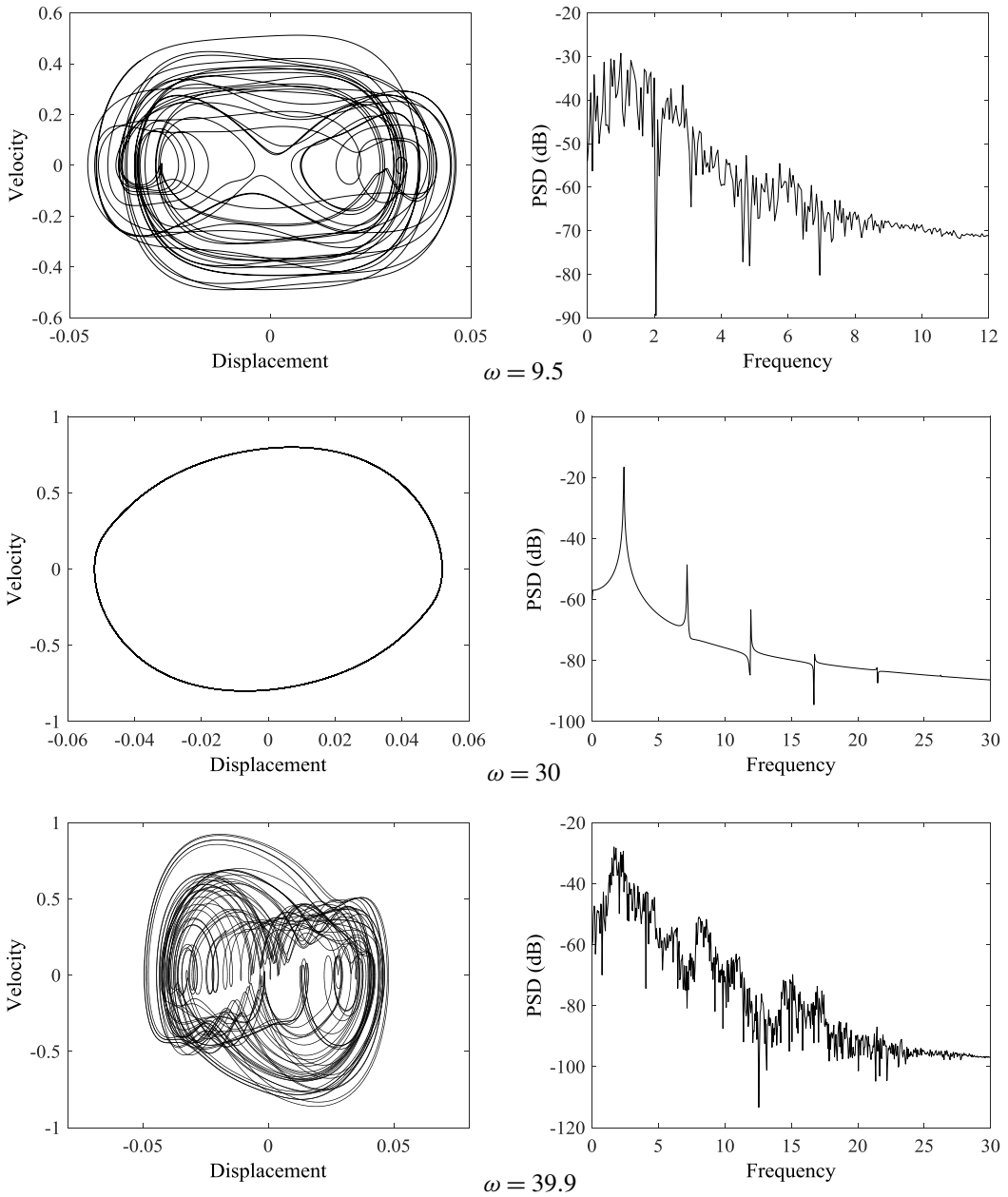
Figure 8. Phase plots and PSD diagrams for the system with motion constraints for $u_0 = 4.5$ and three values of ω.

back and forth within the gap, showing periodic motions (Figure 8, middle, and Figure 9, middle and bottom), chaotic-like motions (top parts of Figures 8 and 9) and transition motions (Figure 8, bottom) at some particular pulsating frequencies. The Poincaré maps for period-1 and multiperiod motions, as well as chaotic motions are constructed and shown in Figure 10. In this figure, the number of points in
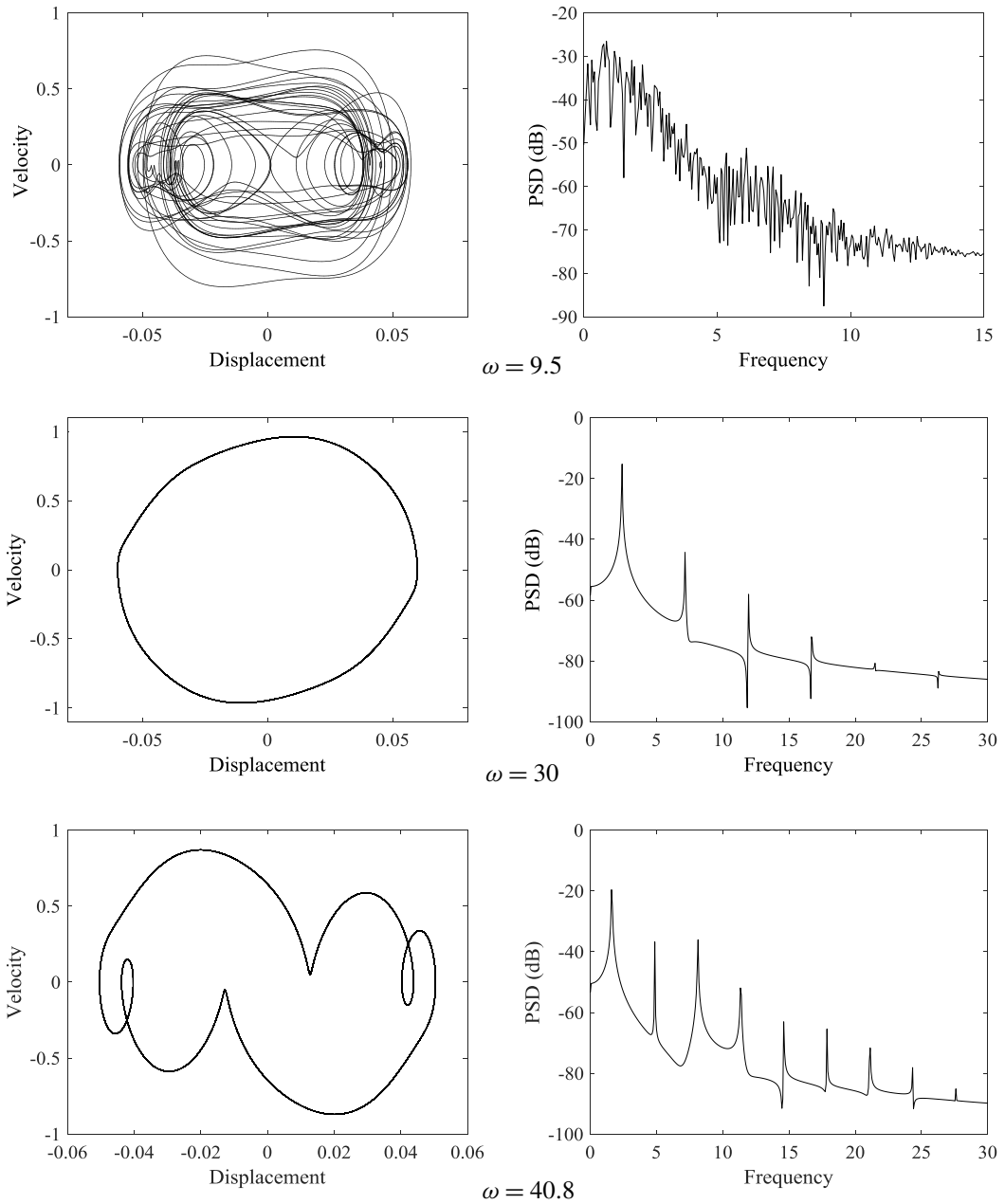
Figure 9. Phase plots and PSD diagrams for the system with motion constraints for $u_0 = 6$ and three values of ω.

Poincaré maps is twice as big as the number of pulsating period [Cai and Chen 1993]. Thus, the Poincaré maps for period-1, period-2, and chaotic motions consist of two points, four points, and infinitely many points, respectively, as seen in Figure 10. It is seen that the Poincaré map for chaos shows a complex fractal structure.
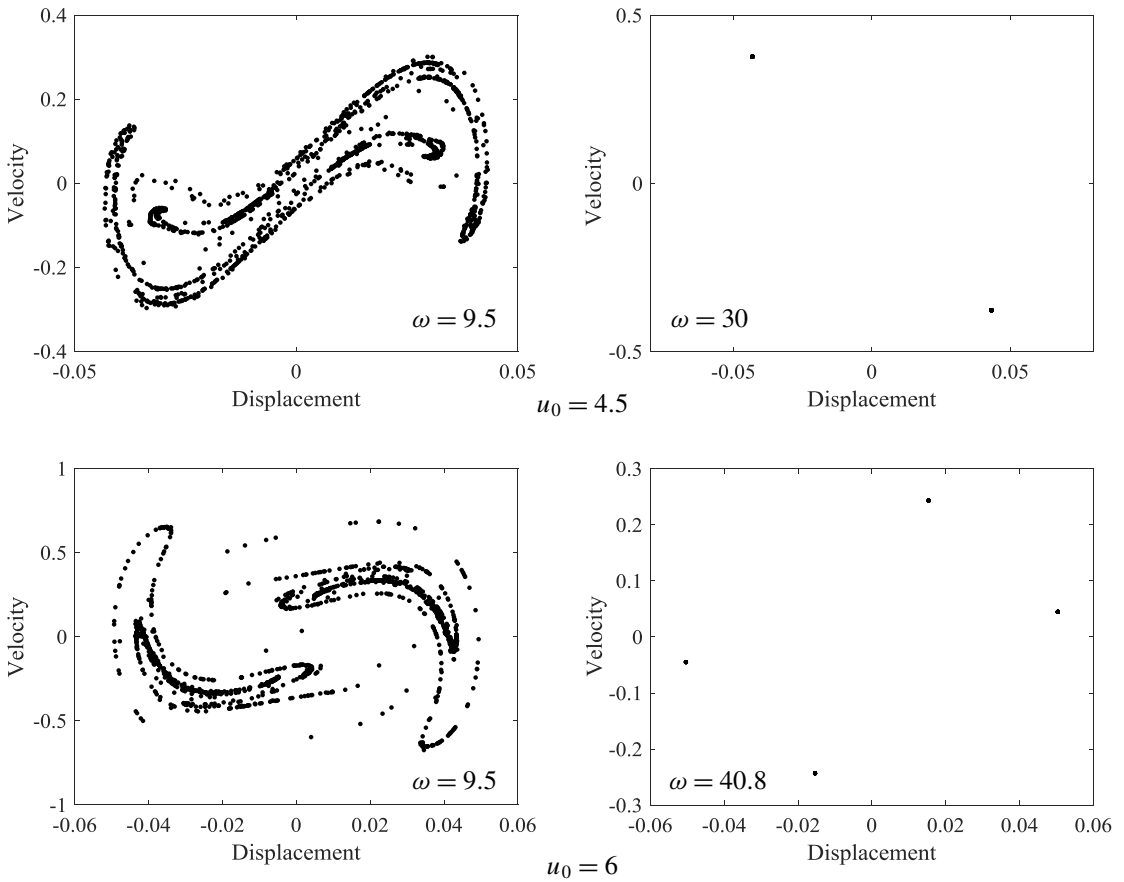
Figure 10. Poincaré maps for chaotic, period-1 and multiperiod motions.

Figure 11 shows mode shapes of the pipe for two sets of system parameters with different mean flow velocities and pulsating frequencies. To make the oscillation style clearer, only half-period of the motion is presented since it is a periodic vibration. We can see two phenomena from these mode shapes. The first is that the pipe deflects like a sinusoidal function in a period when it crosses the straight equilibrium position. The second is when the pipe bangs on one constraint, the impacting force makes the pipe rebound from it. Thus, the mode shape also changes at this moment. The time traces shown in Figure 11, right, imply that the difference between the cases of low and high mean flow velocities is obvious.

3.4. *Evolution of the impacting forces between the pipe and constraints.* The previous three subsections have focused on the dynamical behavior of the pipe. We now turn our attention to the evolution of the impacting forces as the pipe is impacting on the constraints. In Figure 1, two contact modes have been shown and there may be some other types in describing the contact behavior. Since the aforementioned two types of contact behavior have been realized in the numerical computation, the impacting force will be presented. The impacting forces may vary dynamically with time since the contact process changes quickly as time progresses.
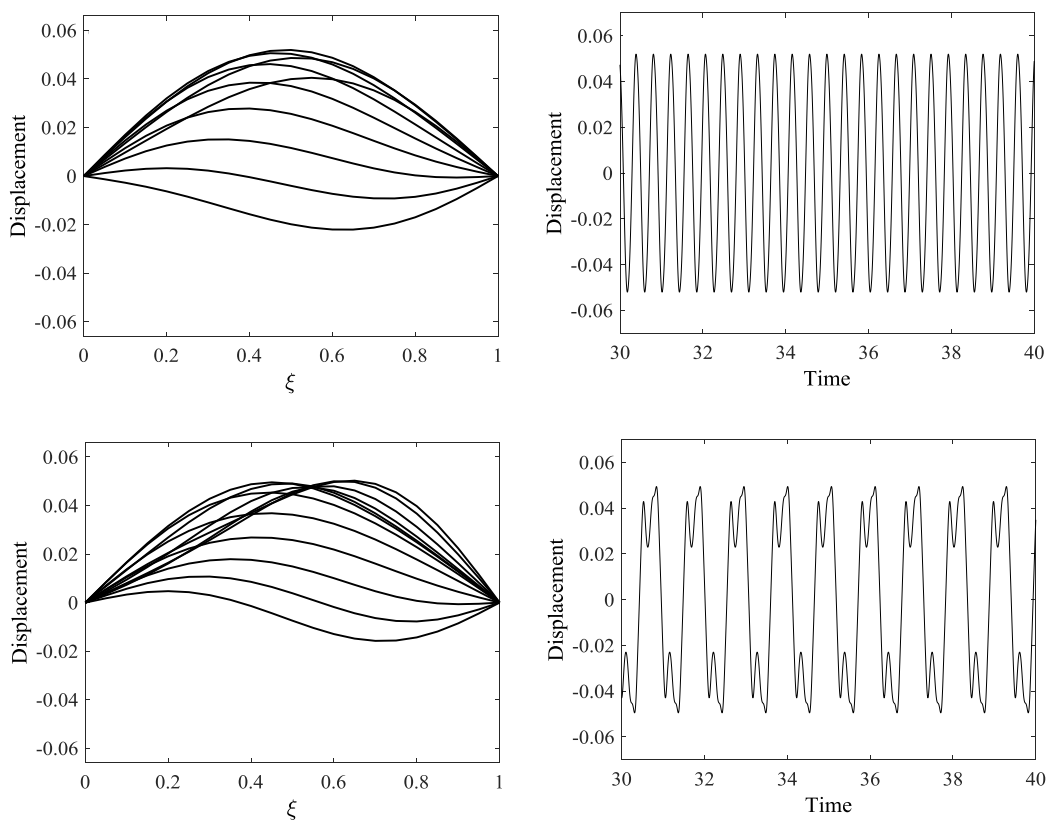
Figure 11. Special vibration shapes and displacement responses at the mid-point of the pipe under various load cases. (a) vibration shape for $u_0 = 4.5$, $\omega = 30$; (b) vibration shape for $u_0 = 6$, $\omega = 11.9$; (c) displacement for $u_0 = 4.5$, $\omega = 30$; (d) displacement for $u_0 = 6$, $\omega = 11.9$.

Inspecting Figure 5, top left, it is found that the buckling amplitude is smaller than the gap between the pipe and constraints and hence no contact occurs in this case. For the results shown in the rest of Figure 5, however, there exist contact forces between the pipe and constraints. These contact forces are further illustrated in Figure 12. As seen in part (a) of the figure, that impacting force appears at one side of the pipe, indicating that the pipe sticks to one of the motion constraints, as also schematically shown in Figure 1, middle. The mode shape of the pipe schematically shown in Figure 1, bottom might be linked to the distributed impacting force represented in Figure 12(c). The distributed impacting force shown in Figure 12(b), however, can be regarded as the transition state from Figure 12(a) to Figure 12(c). As the flow velocity increases from 19.5 to 20, therefore, buckling style of the pipe would change.

4. Conclusions

In this paper, the nonlinear dynamics of a simply supported pipe conveying pulsating fluid is numerically investigated, with consideration of the effect of distributed motion constraints along the axial direction.
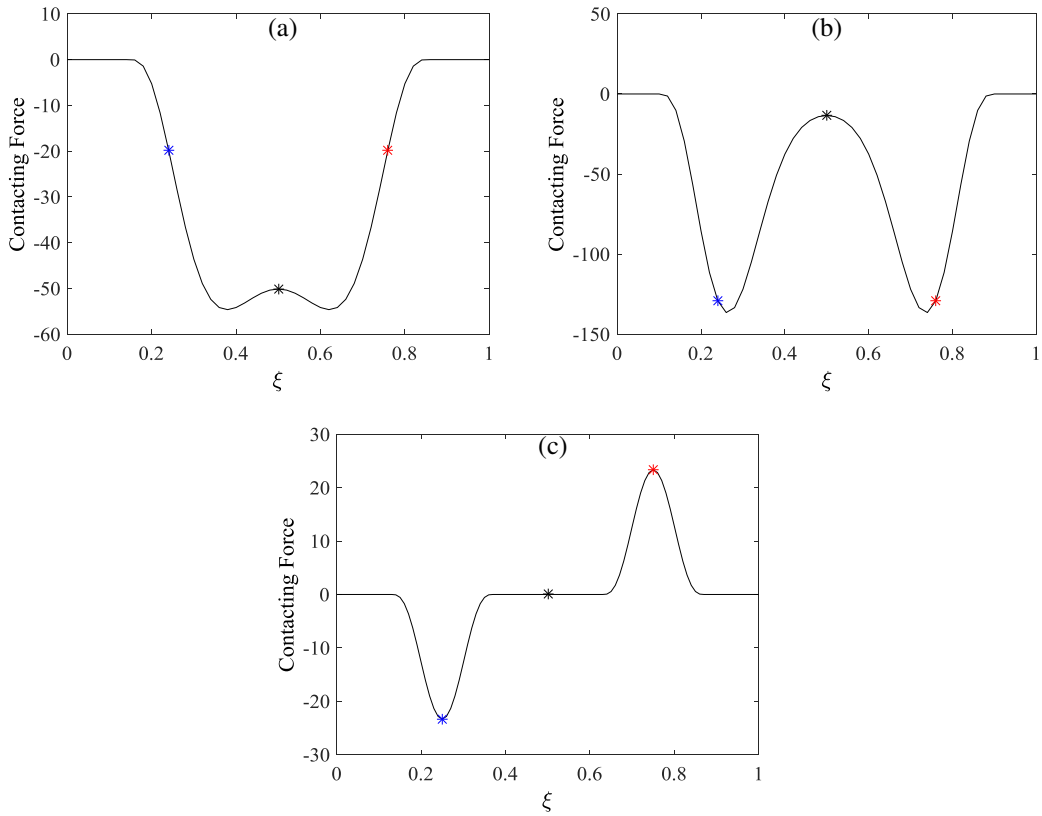
Figure 12. Contacting forces of the distributed motion constraints corresponding to the buckling styles shown in the middle and bottom parts of Figure 1.

The motion constraints are modeled by trilinear springs. The flow velocity is assumed to be pulsatile. A parametric analysis is conducted of the effect of the pulsating frequency and motion constraints on the dynamical behavior of the pipe.

Buckling analysis for a pipe conveying steady fluid flow is conducted first in the presence of distributed motion constraints. The pipe represents four different buckling types within the considered range of flow velocity. Then the significant effect of motion constraints on the flow-induced vibration of the pipe with pulsating fluid is explored. It is shown that the pipe is capable of displaying both periodic and chaotic motions with increasing the pulsating frequency. It is of particular interest to note that the distributed impacting force between the pipe and constraints may be associated with the buckling types of the system. Thus, the present configuration of pipes conveying pulsating fluid flow in the presence of distributed motion constraints serves as an example of a physical system on which the kaleidoscopical dynamical behavior could be observed.

References

[Ariaratnam and Sri Namachchivaya 1986] S. T. Ariaratnam and N. Sri Namachchivaya, "Dynamic stability of pipes conveying pulsating fluid", *J. Sound Vib.* **107**:2 (1986), 215–230.

[Cai and Chen 1993] Y. Cai and S.-S. Chen, "Chaotic vibrations of nonlinearly supported tubes in cross-flow", *J. Press. Vessel Technol.* (*ASME*) **115**:2 (1993), 128–134.

[Chang and Chen 1994] C. O. Chang and K. C. Chen, "Dynamics and stability of pipes conveying fluid", *J. Press. Vessel Technol.* (*ASME*) **116**:1 (1994), 57–66.

[Chen 1971] S.-S. Chen, "Dynamic stability of tube conveying fluid", *J. Eng. Mech. Div.* (*ASCE*) **97**:5 (1971), 1469–1485.

[Chen 1987] S.-S. Chen, *Flow-induced vibration of circular cylindrical structures*, Hemisphere, Washington, DC, 1987.

[Chen 1991] S.-S. Chen, "A review of dynamic tube-support interaction in heat exchanger tubes", pp. 111–120 in *Flow induced vibrations* (Brighton, UK, 1991), IMechE Conf. Publ. **1991-6**, Mech. Engin. Publ., Suffolk, 1991.

[Dai et al. 2014a] H. L. Dai, A. Abdelkefi, and L. Wang, "Modeling and nonlinear dynamics of fluid-conveying risers under hybrid excitations", *Int. J. Eng. Sci.* **81** (2014), 1–14.

[Dai et al. 2014b] H. L. Dai, L. Wang, Q. Qian, and Q. Ni, "Vortex-induced vibrations of pipes conveying pulsating fluid", *Ocean Eng.* **77** (2014), 12–22.

[Ginsberg 1973] J. H. Ginsberg, "The dynamic stability of a pipe conveying a pulsatile flow", *Int. J. Eng. Sci.* **11**:9 (1973), 1013–1024.

[Hassan et al. 2005] M. A. Hassan, D. S. Weaver, and M. A. Dokainish, "A new tube/support impact model for heat exchanger tubes", *J. Fluid. Struct.* **21**:5-7 (2005), 561–577.

[Hu et al. 2016] K. Hu, Y. K. Wang, H. L. Dai, L. Wang, and Q. Qian, "Nonlinear and chaotic vibrations of cantilevered micropipes conveying fluid based on modified couple stress theory", *Int. J. Eng. Sci.* **105** (2016), 93–107.

[Jayaraman and Narayanan 1996] K. Jayaraman and S. Narayanan, "Chaotic oscillations in pipes conveying pulsating fluid", *Nonlinear Dyn.* **10**:4 (1996), 333–357.

[Jin and Song 2005] J. D. Jin and Z. Y. Song, "Parametric resonances of supported pipes conveying pulsating fluid", *J. Fluid. Struct.* **20**:6 (2005), 763–783.

[Ni et al. 2014] Q. Ni, Z. Zhang, L. Wang, Q. Qian, and M. Tang, "Nonlinear dynamics and synchronization of two coupled pipes conveying pulsating fluid", *Acta Mech. Solida Sin.* **27**:2 (2014), 162–171.

[Ni et al. 2015] Q. Ni, Y. Wang, M. Tang, Y. Luo, H. Yan, and L. Wang, "Nonlinear impacting oscillations of a fluid-conveying pipe subjected to distributed motion constraints", *Nonlinear Dyn.* **81**:1-2 (2015), 893–906.

[Païdoussis 1983] M. P. Païdoussis, "A review of flow-induced vibrations in reactors and reactor components", *Nucl. Eng. Des.* **74**:1 (1983), 31–60.

[Païdoussis 1998] M. P. Païdoussis, *Fluid-structure interactions: slender structures and axial flow, I*, Academic Press, San Diego, 1998.

[Païdoussis and Issid 1974] M. P. Païdoussis and N. T. Issid, "Dynamic stability of pipes conveying fluid", *J. Sound Vib.* **33**:3 (1974), 267–294.

[Païdoussis and Semler 1993] M. P. Païdoussis and C. Semler, "Nonlinear and chaotic oscillations of a constrained cantilevered pipe conveying fluid: a full nonlinear analysis", *Nonlinear Dyn.* **4**:6 (1993), 655–670.

[Païdoussis and Sundararajan 1975] M. P. Païdoussis and C. Sundararajan, "Parametric and combination resonances of a pipe conveying pulsating fluid", *J. Appl. Mech.* (*ASME*) **42**:4 (1975), 780–784.

[Panda and Kar 2007] L. N. Panda and R. C. Kar, "Nonlinear dynamics of a pipe conveying pulsating fluid with parametric and internal resonances", *Nonlinear Dyn.* **49**:1-2 (2007), 9–30.

[Panda and Kar 2008] L. N. Panda and R. C. Kar, "Nonlinear dynamics of a pipe conveying pulsating fluid with combination, principal parametric and internal resonances", *J. Sound Vib.* **309**:3-5 (2008), 375–406.

[Pettigrew et al. 1978] M. J. Pettigrew, Y. Sylvestre, and A. O. Campagna, "Vibration analysis of heat exchanger and steam generator designs", *Nucl. Eng. Des.* **48**:1 (1978), 97–115.

[Sri Namachchivaya 1989] N. Sri Namchchivaya [sic], "Non-linear dynamics of supported pipe conveying pulsating fluid, I: Subharmonic resonance", *Int. J. Non-Linear Mech.* **24**:3 (1989), 185–196.

[Sri Namachchivaya and Tien 1989] N. Sri Namchchivaya [sic] and W. M. Tien, "Non-linear dynamics of supported pipe conveying pulsating fluid, II: Combination resonance", *Int. J. Non-Linear Mech.* **24**:3 (1989), 197–208.

[Tang et al. 2014] M. Tang, Q. Ni, Y. Luo, Y. Wang, and L. Wang, "Flow-induced vibration of curved cylinder arrays subject to loose support", *Nonlinear Dyn.* **78**:4 (2014), 2533–2545.

[Wang 2009] L. Wang, "A further study on the non-linear dynamics of simply supported pipes conveying pulsating fluid", *Int. J. Non-Linear Mech.* **44**:1 (2009), 115–121. Correction in **45**:3 (2010) 331–335.

[Wang et al. 2016] L. Wang, Y. Z. Hong, H. L. Dai, and Q. Ni, "Natural frequency and stability tuning of cantilevered CNTs conveying fluid in magnetic field", *Acta Mech. Solida Sin.* **29**:6 (2016), 567–576.

[Weaver et al. 2000] D. S. Weaver, S. Ziada, M. K. Au-Yang, S.-S. Chen, M. P. Païdoussis, and M. J. Pettigrew, "Flow-induced vibrations in power and process plant components: progress and prospects", *J. Press. Vessel Technol.* (*ASME*) **122**:3 (2000), 339–348.

[Xia and Wang 2010] W. Xia and L. Wang, "The effect of axial extension on the fluidelastic vibration of an array of cylinders in cross-flow", *Nucl. Eng. Des.* **240**:7 (2010), 1707–1713.

[Yoshizawa et al. 1986] M. Yoshizawa, H. Nao, E. Hasegawa, and Y. Tsujioka, "Lateral vibration of a flexible pipe conveying fluid with pulsating flow", *Bull. Jpn. Soc. Mech. Eng.* **29**:253 (1986), 2243–2250.

WANG YIKUN: wykfang1053@hust.edu.cn
Department of Mechanics, Huazhong University of Science and Technology, Wuhan, 430074, China

NI QIAO: niqiao@hust.edu.cn
Department of Mechanics, Huazhong University of Science and Technology, Wuhan, 430074, China

WANG LIN: wanglindds@hust.edu.cn
Department of Mechanics, Huazhong University of Science and Technology, Wuhan, 430074, China

LUO YANGYANG: 123443887@qq.com
Department of Mechanics, Huazhong University of Science and Technology, Wuhan, 430074, China

YAN HAO: 824174017@qq.com
Department of Mechanics, Huazhong University of Science and Technology, Wuhan, 430074, China

JOURNAL OF MECHANICS OF MATERIALS AND STRUCTURES

Cover photo: Wikimedia Commons

Journal of Mechanics of Materials and Structures